Am J Physiol Regul Integr Comp Physiol 314: R84–R93, 2018.
First published September 6, 2017; doi:10.1152/ajpregu.00024.2017.

RESEARCH ARTICLE | *Respiration*

Hemoglobin polymerization via disulfide bond formation in the hypoxia-tolerant turtle *Trachemys scripta*: implications for antioxidant defense and O_2 transport

Asbjørn G. Petersen,[1] Steen V. Petersen,[2] Sebastian Frische,[2] Srdja Drakulic,[2] Monika M. Golas,[2] Bjoern Sander,[3] and Angela Fago[1]

[1]*Department of Bioscience, Aarhus University, Aarhus, Denmark;* [2]*Department of Biomedicine, Aarhus University, Aarhus, Denmark; and* [3]*Centre for Stochastic Geometry and Advanced Bioimaging, Aarhus University, Aarhus, Denmark*

Submitted 24 January 2017; accepted in final form 30 August 2017

Petersen AG, Petersen SV, Frische S, Drakulic S, Golas MM, Sander B, Fago A. Hemoglobin polymerization via disulfide bond formation in the hypoxia-tolerant turtle *Trachemys scripta*: implications for antioxidant defense and O_2 transport. *Am J Physiol Regul Integr Comp Physiol* 314: R84–R93, 2018. First published September 6, 2017; doi:10.1152/ajpregu.00024.2017.—The ability of many reptilian hemoglobins (Hbs) to form high-molecular weight polymers, albeit known for decades, has not been investigated in detail. Given that turtle Hbs often contain a high number of cysteine (Cys), potentially contributing to the red blood cell defense against reactive oxygen species, we have examined whether polymerization of Hb could occur via intermolecular disulfide bonds in red blood cells of freshwater turtle *Trachemys scripta*, a species that is highly tolerant of hypoxia and oxidative stress. We find that one of the two Hb isoforms of the hemolysate HbA is prone to polymerization in vitro into linear flexible chains of different size that are visible by electron microscopy but not the HbD isoform. Polymerization of purified HbA is favored by hydrogen peroxide, a main cellular reactive oxygen species and a thiol oxidant, and inhibited by thiol reduction and alkylation, indicating that HbA polymerization is due to disulfide bonds. By using mass spectrometry, we identify Cys5 of the α^A-subunit of HbA as specifically responsible for forming disulfide bonds between adjacent HbA tetramers. Polymerization of HbA does not affect oxygen affinity, cooperativity, and sensitivity to the allosteric cofactor ATP, indicating that HbA is still fully functional. Polymers also form in *T. scripta* blood after exposure to anoxia but not normoxia, indicating that they are of physiological relevance. Taken together, these results show that HbA polymers may form during oxidative stress and that Cys5α^A of HbA is a key element of the antioxidant capacity of turtle red blood cells.

oxidative stress; hemoglobin; polymerization; thiol; adaptation

INTRODUCTION

While present occasionally in mammals (34, 39), fish (11), and birds (7), the ability of some vertebrate tetrameric hemoglobins (Hbs) to form large polymers (here the Hb tetramer is considered as the basic polymer-forming unit) via formation of disulfide bonds occurs widely in reptiles, particularly turtles, due to the relatively high content of cysteine (Cys) (32). This thiol-based polymerization is particularly evident in Hb from turtles, as shown in an early survey study of more than 50 turtle species (37). Several studies have focused on the particularly high Cys content and reactivity of turtle Hbs. One of the first species to be investigated, the South American freshwater turtle *Phrynops hilarri*, was found to express Hb with 8–10 accessible thiols per tetramer (33), supporting the formation of mixed disulfides with glutathione (GSH) in vitro (30). As a consequence of the high Hb concentration and of the high Cys content of the Hb, red blood cells (RBCs) in turtles have a very high content of accessible thiols (~25 mM) (18, 30), whereas in other vertebrate species, the reactive thiol group of GSH makes the major contribution (1–3 mM) (18, 24). The thiol reactivity of GSH plays an important role in the defense against toxic reactive oxygen species (ROS) in hypoxia-tolerant species such as freshwater turtles (2, 17), especially when mitochondrial respiration is resumed after episodes of oxygen deprivation (22, 23). Along the same line, the high content of RBC thiols in turtles, principally located on Hb, has been proposed to protect against oxidative stress associated with cycles of hypoxia and reoxygenation regularly experienced by these species (30, 31), especially due to the presence of mitochondria, a major source of ROS, in their RBCs (24). During oxidative stress, the most abundant of cellular ROS hydrogen peroxide (H_2O_2) (36) can readily react with an accessible thiol group (R-SH) and perform a two-electron oxidation to generate sulfenic acid (R-SOH) (29), which can be further oxidized to sulfinic acid (R-SO_2H) and irreversibly to sulfonic acid (R-SO_3H). However, the sulfenic acid group may also react with a nearby available free thiol to form a disulfide bond (26). This process leads to the formation of a disulfide bond between two GSH molecules to form oxidized GSSG during cellular oxidative stress and contributes to neutralize potentially toxic H_2O_2. GSSG is subsequently reduced to GSH by the NADPH-dependent GSH reductase, thus completing the redox cycle (22). By a similar mechanism, reactive thiol groups located on turtle Hb may react with H_2O_2 to generate disulfide bonds and thus function as an effective redox-buffering system to neutralize H_2O_2 and avoid irreversible inactivation of enzymes and structural proteins by unspecific oxidation (32). In addition to the high thiol content in RBCs, turtles in general possess high constitutive levels of ROS scavenging antioxidant enzymes in tissues (14).

Although it is generally accepted that thiols of Hb enhance antioxidant capacity in turtles, it is yet unclear whether Hb polymerization may affect O_2 binding (39) or RBC shape, as

Address for reprint requests and other correspondence: A. Fago, Dept. of Bioscience, Aarhus University, C. F. Møllers Allé 3, DK-8000 Aarhus C, Denmark (e-mail: angela.fago@bios.au.dk).

known for the sickle cell mutant of human Hb (12). If thiol groups in turtle Hb undergo cycles of oxidation and reduction following oxidative stress episodes, then these processes must not interfere with O_2 transport and cellular integrity. To address these issues, we investigated the nature of Hb polymerization in one of the very few vertebrates able to tolerate prolonged anoxia, the freshwater turtle *Trachemys scripta*. This species is able to survive winter months covered by frozen mud and without access to air (41), yet without significant oxidative damage when it resumes respiration in the spring (14). In terms of its Hb system, *T. scripta* expresses two well-characterized Hb isoforms with similar O_2 binding properties: HbA ($\alpha^A{}_2\beta_2$) and HbD ($\alpha^D{}_2\beta_2$) (8). The primary structure reveals the presence of two Cys residues in the α^A-subunit (position 5 and 104), one Cys residue in the α^D-subunit (position 104) and three Cys residues in the β-subunit (position 23, 93, and 126) (8). Of these, however, only one Cys residue per subunit in each of the two Hb isoforms appears accessible to the solvent (8). As Hb polymerization has been described for this species (37), we examine here in detail the molecular basis for Hb polymerization in *T. scripta* and show that polymerization is mediated by intermolecular disulfide bond formation between subunits of HbA. In combination with analysis of electrophoretic and O_2 binding properties, this indicates that HbA polymerization into a large molecular complex reflects Hb-mediated antioxidant capacity in this extreme vertebrate without impairing O_2 transport.

MATERIALS AND METHODS

Animals, blood samples, and hemolysate. Adult red-eared sliders (*Trachemys scripta*) were kept at 25°C in aquaria at the animal care facility at Zoophysiology, Aarhus University. Blood was collected by cardiac puncture of euthanized (1 ml, 20% pentobarbital sodium) animals after the plastron was removed, as described earlier (8). Hemolysate was prepared using standard procedures and stored in aliquots at −80°C. All procedures were in accordance with the regulation of animal care and experimentation in Denmark, and protocols were approved by the Animal Experimentation Board. All chemicals were from Sigma Aldrich, unless otherwise stated.

Hemoglobin purification. Separation of the hemolysate into HbA and HbD isoforms was achieved by anion-exchange chromatography using an ÄKTA Pure System (GE Healthcare) and a HiTrap Q 5-ml column (GE Healthcare) equilibrated in 10 mM Tris·HCl, and 0.5 mM EDTA, pH 8.3. The two isoHbs were separated using a linear gradient of 0–400 mM NaCl over 30 min at a flow rate of 1 ml/min. Notably, this procedure also removes RBC ATP (a major allosteric cofactor of turtle Hbs) (1, 8) as well as endogenous reducing agents and enzymes. Purified Hbs were dialyzed against 10 mM HEPES, pH 7.6 at 4°C using a slide-a-lyzer (Thermo Scientific) and concentrated by ultrafiltration (4-ml Amicon, 10-kDa cutoff) (Millipore) to a final heme concentration of 1.6–2.5 mM, measured using extinction coefficients for oxy Hb of 14.37 $mM^{-1}\cdot cm^{-1}$ (542 nm) and 15.37 $mM^{-1}\cdot cm^{-1}$ (575 nm) (42). Samples were then stored at −80°C until further use. The duration of the entire procedure from loading the hemolysate onto the anion exchange column to storage of the concentrated isoHbs lasted ~8–12 h. No significant heme ferric (met) oxidation was detected, as estimated from the lack of the absorbance peak at 630 nm. The purity of separated Hbs was subsequently verified by isoelectric focusing (pH 3–9) using the PhastSystem (GE Healthcare).

Size-exclusion chromatography. The apparent molecular weight of each of the isolated Hbs was determined by size-exclusion chromatography using a Superdex 200 10/300 GL column (GE Healthcare) equilibrated in 50 mM Tris·HCl and 0.15 M NaCl, pH 6.0 or 8.0 (to identify possible pH effects), at a flow rate of 0.5 ml/min using an ÄKTA Pure System (GE Healthcare). Absorption was monitored at 280 and 415 nm (to identify heme proteins). The column was calibrated using molecular mass standard containing blue dextran (>2,000 kDa, void volume), ferritin (440 kDa), aldolase (158 kDa), conalbumin (75 kDa), and ovalbumin (43 kDa) (GE Healthcare). Human HbA (64 kDa) was used to evaluate the elution volume of a tetrameric Hb, as vertebrate Hbs show a lower apparent molecular weight on size-exclusion chromatography due to partial dissociation (6, 38, 44). Fractions containing Hbs were pooled, dialyzed, and concentrated by ultrafiltration, as described in *Hemoglobin purification*. The polymer-to-tetramer ratio was calculated by peak integration using the Unicorn 6.3 software provided with the ÄKTA Pure System.

Electrophoretic analyses of Hb polymerization. The presence of disulfide-dependent Hb polymerization was investigated by native PAGE in 10–15% gradient gels using a PhastSystem (GE Healthcare). Samples included unfractioned hemolysate and purified HbA and HbD (0.25 mM heme) in 0.1 M HEPES, pH 6.0, before and after incubation with the thiol-reducing agent DTT (1 mM) for 30 min at room temperature.

The effect of H_2O_2 on Hb polymerization was assessed by using the same electrophoretical technique on 4–15% gradient gels. Samples of polymerized HbA (1 mM heme) were first incubated in 10 mM HEPES and 0.5 mM EDTA, pH 7.4, containing 1 mM DTT (to recover tetrameric Hb) for 30 min at room temperature. After incubation, DTT was removed from the samples by dialysis and tetrameric HbA was then incubated for 30 min at room temperature with H_2O_2 at concentrations of 0–10 mM. To confirm that polymerization occurs via disulfide bonds, dialyzed reduced samples (containing tetrameric HbA) were incubated with 10 mM HEPES and 0.5 mM EDTA, pH 7.4, containing 100 mM *N*-ethylmaleimide (NEM) for 1 h to block reactive Cys and then treated with H_2O_2 (0–10 mM) for 30 min at room temperature. The final heme concentration for all samples was 0.25 mM heme. H_2O_2 concentration in stock solutions was determined spectrophotometrically at 240 nm using a molar extinction coefficient of 39.4 $M^{-1}\cdot cm^{-1}$ (15).

For analysis of HbA and HbD subunit composition, proteins were denatured and subjected to SDS-PAGE using 10% polyacrylamide gels and the glycine/2-amino-2-methyl-1,3-propanediol-HCl buffer system (3). For analysis of proteins under reducing conditions, the samples were boiled in the presence of 0.5% (wt/vol) SDS and 50 mM DTT before electrophoresis. All gels were stained with Coomassie brilliant blue.

Separation of Hbs subunits by reverse-phase chromatography. Purified HbA and HbD were acidified by the addition of 0.1% trifluoroacetic acid (TFA) and α^A- and α^D-chains were separated from β-chains, respectively, by reverse-phase UPLC using a Waters BEH300 C4 column (2.1 × 150 mm; 1.7 μm) operated by an Acquity UPLC system (Waters). The column was developed at a flow rate of 200 μl/min using a 0.6% min^{-1} linear gradient of 90% acetonitrile and 0.08% (vol/vol) TFA (solvent B) in 0.1% (vol/vol) TFA (solvent A). Eluted protein was monitored by absorption at 220 nm, and fractions were collected manually. For subsequent analysis by SDS-PAGE (as described in *Electrophoretic analyses of Hb polymerization*), fractions were lyophilized and resuspended in 50 mM Tris·HCl, pH 7.4 containing 5 mM iodoacetamide to block free thiols.

Mass spectrometric analyses. For analysis by in-gel digestion, individual bands from SDS-PAGE were excised and prepared for digestion using porcine trypsin (Promega) as described previously (35). Generated peptides were recovered by reverse-phase absorption (StageTips, C18; Thermo Scientific) and eluted directly onto a stainless steel matrix-assisted laser desorption/ionization time-offlight (MALDI) target plate by using α-cyano-4-hydroxycinnamic acid in 70% acetonitrile and 0.1% TFA (4 mg/ml). Peptides were subsequently analyzed in mass spectrometry (MS) and tandem MS (LIFT) using an Autoflex Smartbeam III instrument (Bruker) calibrated using a peptide mixture containing 7 calibrants (PepMix; Bruker). For

analysis of the isolated α^A-subunit, the relevant fraction was lyophilized and resuspended in 50 mM ammonium bicarbonate, containing 5 mM iodoacteamide to block free thiols and prevent disulfide shuffling. The material was added porcine trypsin (Promega) in an estimated ratio of 1:40 and incubated 30 min at 37°C. Generated peptides were recovered by reverse-phase absorption and analyzed by MALDI-MS as described above. All spectra were interrogated by using the GPMAW software (Lighthouse Data, Denmark).

Electron microscopy. Electron microscopy was performed to visualize the Hb aggregates. The sandwich carbon-negative staining method was used (5). In detail, the incubation of a carbon film with 26 μl of Hb (1.58 mM) was followed by a wash with H_2O and incubation with freshly made 2% uranyl formate. The carbon film with the sample was absorbed to a Maxtaform HR26 Cu/Rh EM grid (EMS), and after a short drying, the grid was transferred into a new well filled with 106 μl uranyl formate and a floating carbon film. Before being air dried, excess stain was blotted with Whatman filter paper (Sigma-Aldrich). The images were recorded in a 120-kV electron microscope (FEI) with a MultiScan 794 CCD camera (Gatan, Pleasanton) at a magnification of ×52,000 and analyzed with ImageJ v. 1.49 (National Institutes of Health).

O_2 equilibria. O_2 equilibrium curves of HbA were measured in 5-μl samples at 0.2 mM heme concentration in 0.1 M HEPES buffer, pH 7.4 at 20°C, in the absence and presence of 1 mM DTT to reduce disulfide bonds. Curves were measured using a modified diffusion chamber connected to Wösthoff gas mixing pumps described earlier (8, 43, 44). O_2 affinity (measured as P_{50}, the P_{O_2} at half-saturation) and cooperativity (measured as Hill coefficient n) for each curve were derived by nonlinear fitting regression of O_2 fractional saturation (S_{O_2}) vs. O_2 tension (P_{O_2}) according to the Hill equation $S_{O_2} = P_{O_2}{}^n / (P_{50}{}^n + P_{O_2}{}^n)$ using the SigmaPlot 11 software (Systat Software) (19, 20, 40). Values of P_{50} and n_{50} (reported as means ± SE) were calculated from five saturation points per curve. Significant differences ($P \leq 0.05$) were evaluated by one-way ANOVA followed by Bonferroni *t*-test using the SigmaPlot 11 software.

Light microscopy. RBC shape alterations induced by H_2O_2 were examined using light differential interference contrast microscopy. RBCs were prepared as previously described (13). Briefly, cell suspensions were made by addition of 1 μl of blood to 40 μl plasma containing 0, 0.5, and 10 mM H_2O_2. A droplet of the cell suspension was then placed on a glass slide, enclosed with a circular glass cover, and observed over time on a Leica DMIRE2 microscope equipped with a SP2 laser scanning confocal (Leica Microsystems; using a HCX PL APO 63x/1.32–0.6 oil immersion lens and differential interference contrast prism). Excitation wavelength was 488 nm and the transmitted light was recorded. Images were viewed using Leica Confocal Software v. 2.61 (Leica Microsystems). Markers for cell shape alteration included a distorted shape and a granular appearance, ascribable to formation of intracellular polymers (21).

Hb polymerization in blood after exposure to anoxia. A standard protocol used previously to expose *T. scripta* to anoxia (18) was used here to test whether polymerization occurred in turtle blood. Blood samples were taken as described in *Animals, blood samples, and hemolysate* or from the neck venous sinus and transferred to Eschweiler tonometers, where they were sequentially equilibrated with air (normoxia, 1 h), pure N_2 (anoxia, 3 h), and air (reoxygenation, 30 min) under constant agitation at room temperature. At the end of each period, a blood aliquot was withdrawn using a gastight syringe and the hemolysate was prepared using a lysis buffer containing 100 mM NEM to stop polymerization. The presence of Hb polymerization was investigated by native PAGE in 4–15% gradient gels. As a control, blood was equilibrated in tonometers with air (normoxia, 4.5 h) at room temperature. Plasma was also run in parallel in native PAGE for comparison.

RESULTS

Anion exchange chromatography of *T. scripta* hemolysate showed two distinct peaks corresponding to pure HbA and HbD, as verified by isoelectric focusing (Fig. 1). Size-exclusion chromatography showed that HbA consists of a major high-molecular weight fraction eluting with the void volume of the column (MW >600) and a minor fraction representing the tetrameric protein, whereas HbD eluted in a single peak corresponding to the tetrameric protein (Fig. 2). Identical elution profiles were obtained at both pH 6.0 and 8.0 (except for a slight increase in the polymer-to-tetramer ratio from 81:19 at pH 6.0 to 86:14 at pH 8.0). Addition of the allosteric cofactor ATP to the elution buffer had no effect on the elution profile of HbA and HbD (data not shown), indicating that polymerization of HbA does not depend on changes in the T-R allosteric equilibrium. As shown in Fig. 2, the high-molecular weight peak of HbA was not symmetric but showed a pronounced tail extending to the tetrameric peak, indicating the presence of large protein polymers with progressively decreasing size. The tetrameric fraction of both Hb isoforms had an apparent molecular weight of 46 rather than the expected of 64–68, thus confirming previous observations of size-exclusion chromatography of vertebrate Hbs (6, 37, 44).

Analysis of untreated hemolysate by native PAGE showed two distinct bands corresponding to the two Hb isoforms (Fig. 3). However, HbA purified by anion-exchange chromatography showed a major high-molecular weight band that did not enter the resolving polyacrylamide gel and a minor band. Treatment of the HbA sample with DTT before electrophoresis removed the high-molecular weight band and produced a band with mobility identical to that of HbA in the hemolysate (Fig. 3). Conversely, purified HbD resolved into a single band having the same mobility as in the hemolysate, regardless of the presence of DTT (Fig. 3). Taken together, these data show that the removal of reducing enzymes and cofactors present in the RBCs during anion-exchange purification and the subsequent Hb processing of several hours caused pronounced

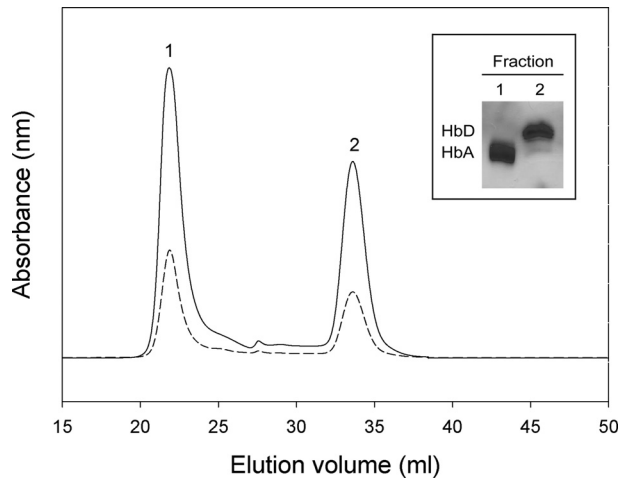

Fig. 1. Separation of turtle hemoglobin (Hb) isoforms. Freshly prepared hemolysate was subjected to anion-exchange chromatography, where it resolved into 2 peaks, corresponding to the 2 Hb isoforms HbA (*fraction 1*) and HbD (*fraction 2*). Elution was monitored at 415 nm (continuous line) and 280 nm (dashed line). The numbered fractions (*fraction 1*, HbA; *fraction 2*, HbD) were collected and their purity verified by isoelectric focusing (*inset*).

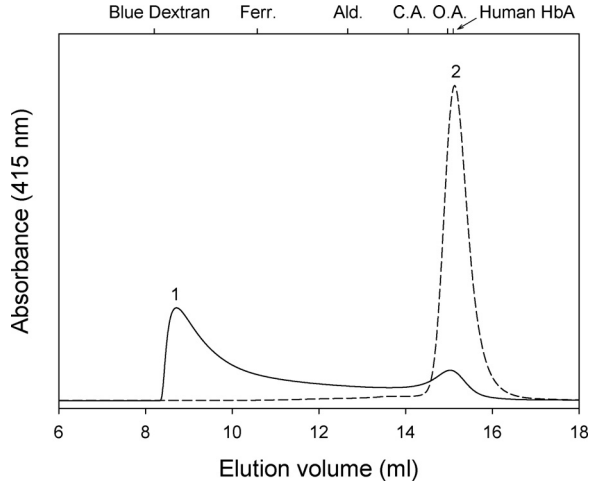

Fig. 2. Size-exclusion chromatography of isolated turtle HbA and HbD. The elution profiles of HbA (continuous line) and HbD (dashed line) are shown, indicating high-molecular weight polymeric (*peak 1*) and tetrameric (*peak 2*) assemblies of HbA and tetrameric assembly of HbD. Elution volumes of human HbA, ovalbumin (O.A.), conalbumin (C.A.), aldolase (Ald.), ferritin (Ferr.), and blue dextran (void volume) are indicated at the top of the chromatogram.

polymerization of HbA via formation of disulfide bonds, which are reduced by DTT. In contrast, HbD is not prone to polymerization.

To further characterize the nature of polymerization, we subjected purified HbA (mostly polymer, Fig. 2) and HbD (all tetramer, Fig. 2) to reverse-phase chromatography in order to isolate their respective α- and β-chains. This separation presented two clusters of peaks for each chain in both HbA and HbD, suggesting some subunit heterogeneity (Fig. 4, *A* and *B*). The collected peaks were subjected to SDS-PAGE analysis at both nonreducing (−DTT) and reducing conditions (+DTT) to disrupt disulfides, and bands were identified by in-gel digestion and MS (shown in Fig. 4, *A* and *B*, *insets*). When the fractions containing the α^A-chain (Fig. 4*A*; *fractions 1–4*) were analyzed by SDS-PAGE under nonreducing conditions, the major fraction (*fraction 3*) presented a significant amount of a α^A-α^A-dimer (*band a1* in *fraction* 3, Fig. 4*A*). This was converted to a α^A monomeric band by DTT (*band a5* in *fraction 3*, Fig. 4*A*), showing that the α^A-α^A-dimer is established by an intermolecular disulfide bond. Analysis of fractions representing the α^D-subunit presented a major band representing the monomer at both nonreducing and reducing conditions (*band d2* and *d4* in *fraction 1*, respectively, Fig. 4*B*). Albeit a small fraction of the α^D (*band d1* in *fraction 1*, Fig. 4*B*) migrated as a dimer, this species could not be removed by reduction, indicating that some other cross link can form in a minor population of the protein. Likewise, the major part of the isolated β-subunit migrated as a monomeric band in both HbA and HbD (*fractions 8* and *6* in Fig. 4, *A* and *B*, respectively). In concert, this analysis suggests that the polymerization observed for HbA (Figs. 2 and 3) is supported by an intermolecular disulfide bond established between α^A-subunits of adjacent protein molecules.

To identify the Cys residue(s) involved in disulfide bond formation, we subjected the material collected in reverse-phase chromatography of HbA, *fraction 3*, containing the α^A-α^A-dimer (Fig. 4*A*) to tryptic digestion. The digestion was performed in the presence of iodoacetamide to block any free Cys residues and avoid disulfide bridge shuffling. The digested material was subsequently analyzed under both non-reducing and reducing conditions by using MALDI-MS. By close inspection of the generated spectra, we could detect a peptide of *m/z* 2346.36 under nonreducing conditions that was absent following reduction with DTT (Fig. 5*A*). The observed *m/z* value correlates well with the presence of a disulfide-linked dimeric peptide representing the sequence Val1α^A-Lys11α^A (calculated *m/z* 2346.24), encompassing Cys5α^A. Further analysis by tandem MS showed that this dimer generated three major fragments representing disruption of the disulfide bond, as indicated (25) (Fig. 5*B*), as well as other minor fragments. Since this dimeric peptide encompasses Cys5α^A, this analysis suggests that the ion of *m/z* 2346.36 represents a disulfide-linked homodimeric Val1α^A-Lys11α^A dipeptide. To further corroborate this conclusion, we subjected the sample to reduction using DTT. An ion of *m/z* 1174.64 was detected in the presence of DTT but not in its absence (Fig. 5*C*). This peptide ion corresponds to the α^A-chain NH_2-terminal Val1α^A-Lys11α^A peptide (calculated *m/z* 1174.62), whose sequence was further confirmed by MS/MS analysis (Fig. 5*D*). Collectively, these MS data show that the α^A-chain has the capacity to form homodimers via Cys5α^A.

The structural organization of the HbA polymer was investigated by electron microscopy. By using negative staining of HbA, we observed polymers of variable size (Fig. 6). Intermediate-sized structures having a length of ~50–60 nm and a diameter of ~7 nm appeared linear, whereas largest structures were of irregular shape. Individual structures were also observed, with a diameter of ~5.5 nm, consistent with isolated Hb tetramers (10). The shape and size of the molecular structures visualized indicate that isolated tetrameric HbA forms regular chains (intermediate size) that can either fold or branch out (largest size) into very large polymers (Fig. 6).

To understand whether polymerization affected the O_2 binding properties of HbA, we separated polymer and tetramer

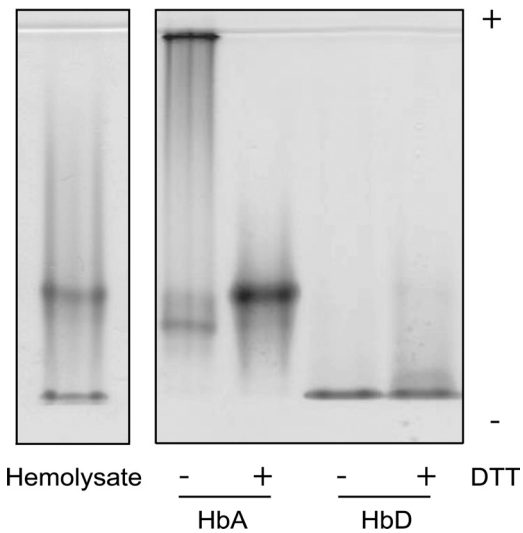

Fig. 3. Effect of the reducing agent DTT on turtle Hb polymerization. Native PAGE analyses of turtle hemolysate and purified HbA and HbD were performed after incubation with DTT, as indicated. PAGE of hemolysate and isolated isoHbs were performed in parallel in the PhastSystem under identical conditions.

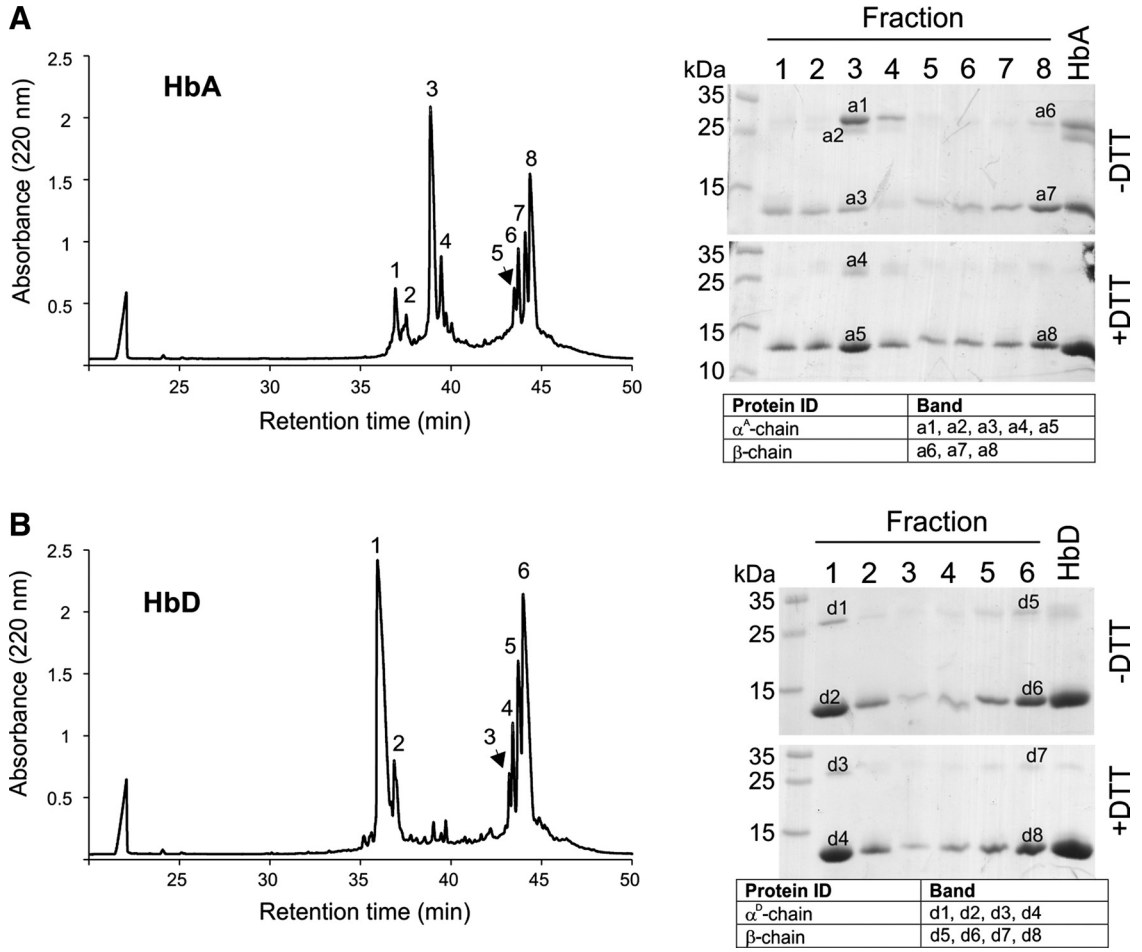

Fig. 4. Separation of α- and β-subunits of turtle HbA and HbD and identification of disulfide bond between α^A chains of HbA. Purified HbA (*A*) and HbD (*B*) were subjected to reverse-phase chromatography and numbered fractions (*1–8* in HbA and *1–6* in HbD) were collected manually (*left*). The heme group eluting at 21.5 min was not collected. The individual fractions were lyophilized and subjected to SDS-PAGE analysis at nonreducing (−DTT) and reducing (+DTT) conditions, as indicated (*right*). Protein was detected by Coomassie Brilliant blue staining and labeled bands were analyzed by mass spectrometry to identify α- and β-chains. The identity of the bands is shown in tables below gels. *Fraction 3* of HbA (*A*) contains a high-molecular weight α^A chain in the absence of DTT (*band a1*, *top*) that disappears with DTT (*band a5*, *bottom*). The SDS-PAGE analysis included purified and unfractionated HbA or HbD (*right lanes*) as well as molecular weight markers (*left lanes*).

fractions by size-exclusion chromatography for O_2 equilibrium measurements. Polymer and tetramer HbA samples showed identical O_2 affinity (Table 1), with P_{50} values of 1.84 and 1.85 Torr, respectively. The same P_{50} (1.87 Torr) was found in experiments performed in the presence of DTT. Addition of ATP to the samples significantly lowered O_2 affinity in polymer and tetrameric HbA fractions, with a P_{50} of 7.92 and 7.55 Torr, respectively, as expected from the allosteric effect of ATP on turtle Hb O_2 affinity (8). Remarkably, all fractions of Hbs were highly cooperative, with n_{50} values between 2.2 and 2.8 (data not shown). Affinity and cooperativity values for polymeric and tetrameric HbA samples (with and without DTT) were statistically not significantly different. These data indicate that the O_2 affinity, cooperativity, and ATP sensitivity of HbA are not affected by formation of polymers via intermolecular disulfide bonds.

Since H_2O_2 is the most abundant ROS in cells (36) and a major cause of disulfide bonds in vivo (26), we investigated the effect of H_2O_2 on HbA polymerization using native PAGE. In these experiments, purified polymeric HbA was first reduced with 1 mM DTT to recover the individual HbA tetramers, and aliquots were then incubated for 30 min with different concentrations of H_2O_2. In the presence of H_2O_2, the band corresponding to the tetrameric HbA disappeared, while a smear with lower electrophoretical mobility, consistent with the formation of linear polymeric chains of increasing size, became evident (Fig. 7). Alkylation of HbA reactive thiols with NEM before incubation with H_2O_2 prevented the formation of a smear in samples treated with H_2O_2, thereby further substantiating that H_2O_2 caused polymerization of HbA via disulfide bonds. Similar results were obtained after incubating polymeric HbA previously reduced by DTT with 0.5 mM H_2O_2 over a time range of 0–240 min (data not shown).

We then tested whether Hb polymerization occurred in *T. scripta* blood when subjected to an anoxia/reoxygenation protocol at room temperature identical to that used for live turtles (18). By using native PAGE of blood lysates after normoxia, anoxia, and reoxygenation, we consistently found formation of high-molecular weight bands in blood samples exposed to anoxia and anoxia/reoxygenation but not to normoxia (Fig. 8). These bands were not present in the plasma (Fig. 8).

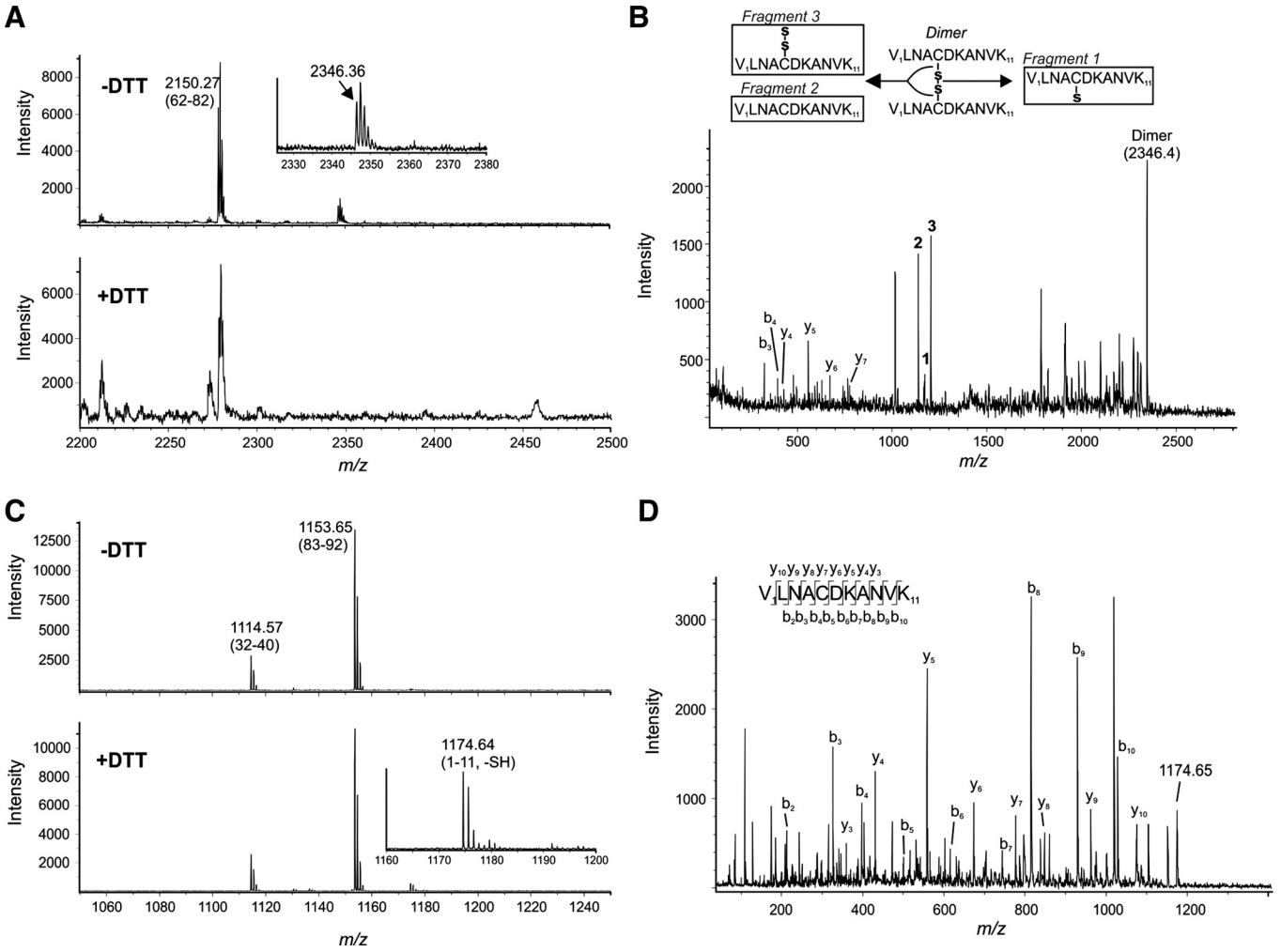

Fig. 5. Identification of the intermolecular disulfide bond between Cys5α^A residues by mass spectrometry. Isolated α^A (shown in Fig. 4*A*, *fraction 3*) was subjected to in-solution digestion using trypsin. Generated peptides were subsequently analyzed by matrix-assisted laser desorption/ionization time-offlight (MALDI) mass spectrometry MS (*A*) under nonreducing (−DTT, *top*) and reducing (+DTT, *bottom*) conditions, i.e., in absence and presence of DTT, respectively. Intervals representing *m/z* in the ranges 2,200–12,500 (*A*) and *m/z* 1,050–1,250 (*B* and *C*) are shown. The dimeric peptide containing the intermolecular disulfide bond with *m/z* 2346.36 is shown in *A* and *B* and the corresponding monomeric peptide after DTT reduction with the expected *m/z* 1174.64 in (C), corresponding to the NH_2-terminal tryptic peptide Val1α^A-Lys11α^A (−SH indicates free thiol). Three major products of the dimeric peptide (numbered 1–3) were generated when the ion was subjected to MS/MS analysis (*B*). These ions are generated by laser-induced cleavage of the disulfide bond as indicated in *B*. In addition, fragment ions of the Val1α^A-Lys11α^A were also detected (*y* and *b* ions indicated). The identity of the reduced Val1α^A-Lys11α^A peptide (+DTT; *C*) was validated by MS/MS analysis producing *y* and *b* ions, as indicated (*D*).

We finally then tested if externally added H_2O_2 caused alterations in RBC shape via polymer formation. *T. scripta* RBCs were incubated with H_2O_2 added to plasma (at final concentrations of 0.5 and 10 mM), and their shape was followed over time (0–3 h) using light microscopy. The majority of the untreated RBCs (i.e., without H_2O_2 added to plasma) had the typical oval and flattened shape (Fig. 9*A*). Over time, RBCs did not change shape and kept their normal smooth surface and clear cytoplasm, regardless of the presence of H_2O_2 (Fig. 9). As RBC appeared to become dry, we stopped monitoring after 3 h of incubation.

DISCUSSION

A major result of this study is the finding that HbA, the major isoHb component of the freshwater turtle *T. scripta*, is prone to spontaneous and extensive polymerization into linear polymeric chains of different size (Figs. 2, 3, and 6). We demonstrate that these linear polymers form via intermolecular disulfide bonds between HbA tetramers, as polymerization is fully reversed by the thiol-reducing agent DTT (Fig. 3), promoted by H_2O_2 (Fig. 7), a known cellular thiol oxidant (26), and inhibited by NEM (Fig. 7), a thiol-alkylating agent. Specifically, disulfide bonds are formed between Cys5α^A of the α^A-subunits of adjacent HbA molecules, as determined by MS (Figs. 4 and 5). Thus, a specific reactive thiol group of turtle HbA may become reversibly oxidized to a disulfide bond, in analogy with the GSH-to-GSSG transition, and may thus contribute to enhancing the thiol-dependent cellular antioxidant defense. Although other Cys residues are present in HbA and appear sufficiently exposed to the surface (8), they do not seem to contribute significantly to HbA polymerization, as we could not identify by MS other peptides containing a disulfide bond. Among reptiles, another example of a Hb forming large polymers due intermolecular disulfide

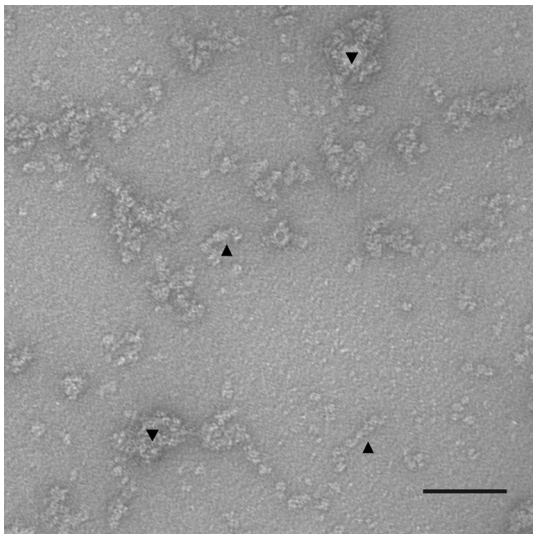

Fig. 6. Electron microscopy image of turtle HbA polymers. The sandwich carbon negative staining method was applied to a sample of purified HbA. Intermediate (▲) and large linear polymeric structures (▼) are highlighted. Scale bar = 60 nm.

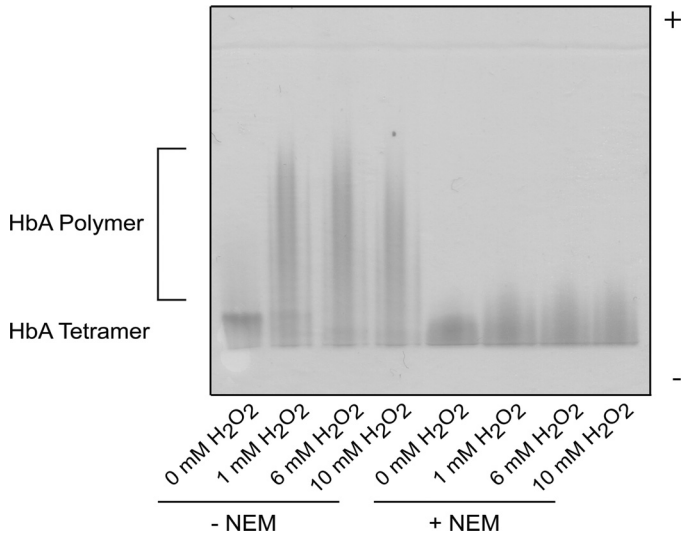

Fig. 7. Effect of H_2O_2 on turtle HbA polymerization. HbA tetramers (prepared by prior reduction with DTT and dialysis) were incubated with H_2O_2 (0–10 mM), as indicated, and run on a native PAGE. The identity of the bands is shown left to the gel. Blocking reduced thiols with *N*-ethylmaleimide (NEM) before H_2O_2 oxidation, as indicated, prevented polymer formation.

bonds is that of the dwarf caiman (44). Based on the amino acid sequence, two external Cys residues in positions 18 and 19 of the α-chain have been proposed to be involved in polymer formation in this Hb (44), indicating variations in the mechanisms of polymerization via disulfide bonds in reptilian Hbs. The reactive Cys5α^A of *T. scripta* HbA is readily oxidized into disulfide bonds when HbA is purified from endogenous reducing agents normally present in RBCs (Fig. 3). Similarly, freshly prepared hemolysate (Fig. 3) and normoxic blood (Fig. 8) show no evidence of polymer formation. In contrast, high-molecular weight polymers start to form after anoxic exposure of turtle blood (Fig. 8), indicating that the polymerization process is physiologically relevant as it takes place in intact RBCs. The somewhat low level of polymers is fully consistent with the presence of antioxidant systems in intact RBCs that would tend to reduce disulfide bonds between HbA tetramers, possibly by a yet unidentified specific NADPH-dependent reductase functionally similar to the GSH reductase. Conversely, these disulfide bonds form massively in vitro when antioxidants are absent (Figs. 2, 3, 6, and 7). Another factor that may contribute to inhibit polymer formation in turtle RBCs after anoxia (Fig. 8) is the concomitant presence of nonpolymerizing HbD, which would interfere with the HbA-HbA interaction and with disulfide formation. Some interaction may also take place between HbA and HbD in the RBC that may prevent HbA polymerization, as it has been observed that the O_2 affinity of the 1:1 mixture of the two Hb isoforms in vitro is lower than for the isolated components, although this aspect remains to be investigated further (13).

As for other tissues, exposing turtle blood to episodes of anoxia would lead to subsequent oxidative stress and increase in ROS in RBCs, due to the presence of mitochondria, with consequent increase in thiol oxidation of HbA (Fig. 8). Accordingly, we find here that HbA polymers are promoted in vitro by H_2O_2 (Fig. 7), a major thiol-oxidizing ROS that forms in tissues in vivo when mitochondria are reoxygenated after hypoxic episodes (36). Incubation of turtle blood with H_2O_2 even at high concentration (Fig. 9), however, does not cause

Table 1. *Oxygenation properties of Trachemys scripta HbA tetramer and polymer*

	P_{50}, Torr	
	Stripped	0.15 mM ATP
$HbA_{tetramer}$	1.84 ± 0.03	7.55 ± 0.25
$HbA_{polymer}$	1.85 ± 0.13	7.92 ± 0.27
HbA_{DTT}	1.87 ± 0.00	

Values are expressed as means ± SE. Conditions are as follows: 0.1 M HEPES, pH 7.4, 20°C, in the absence and presence of 1 mM DTT. P_{50}, O_2 affinity; $HbA_{tetramer}$, hemoglobin isoform A tetramer; $HbA_{polymer}$, hemoglobin isoform A polymer; HbA_{DTT}, hemoglobin isoform A treated with DTT.

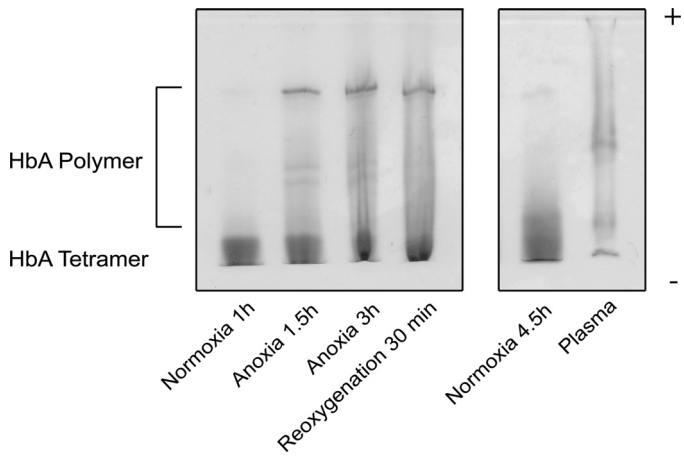

Fig. 8. Turtle Hb polymerization in blood following exposure to anoxia. Blood samples were subjected to a standard anoxia/reoxygenation protocol used for live turtles and hemolysates were prepared from blood aliquots taken at the end of each incubation period, as indicated, using NEM-containing buffer. Samples were analyzed by native PAGE along with normoxic samples (control) and plasma. The identity of the bands is shown on the *left*. Gels were run in parallel in the PhastSystem under identical conditions.

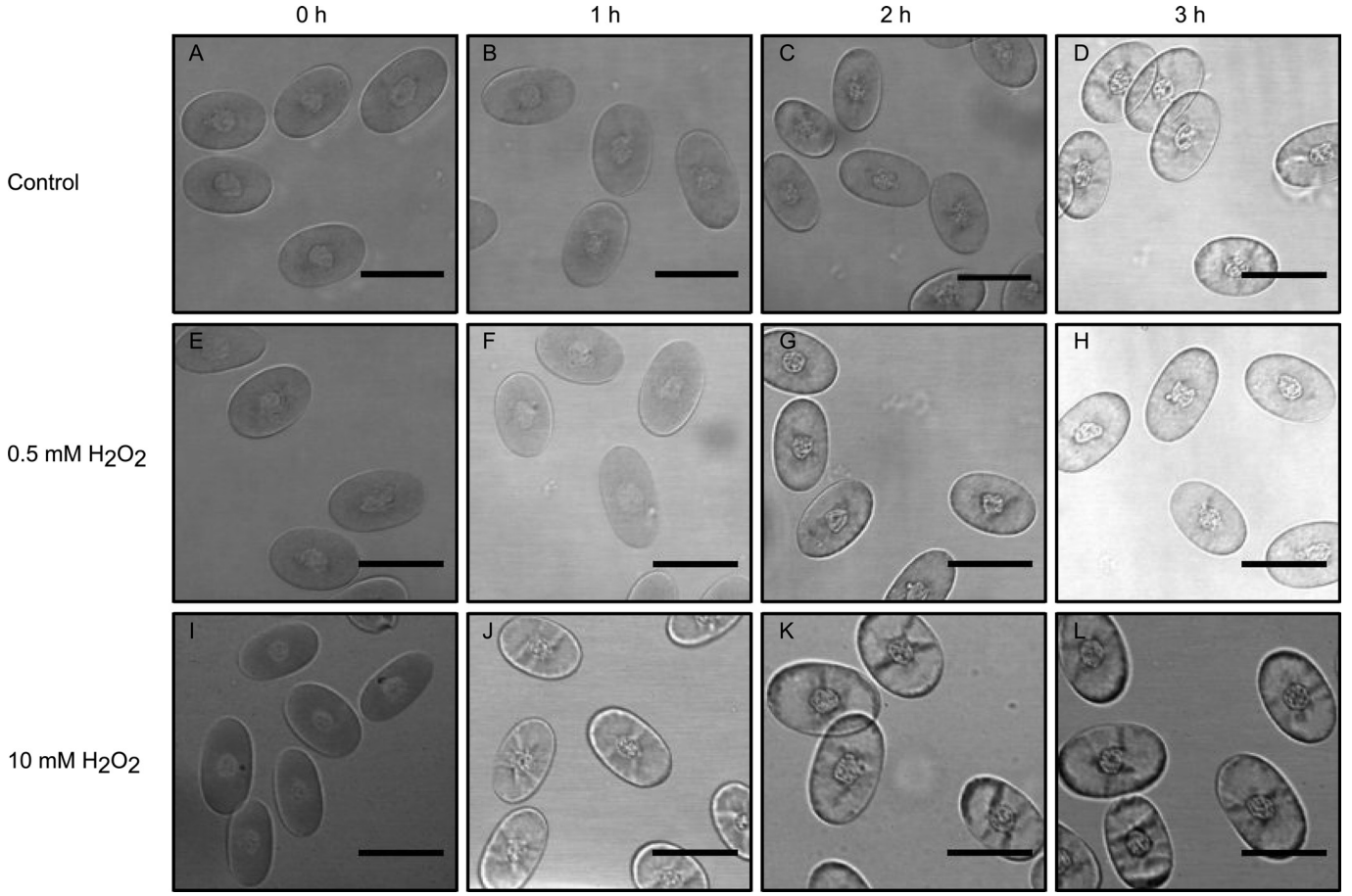

Fig. 9. Light microscopy of turtle red blood cells (RBCs) exposed to H_2O_2. Isolated RBCs were incubated with plasma containing H_2O_2, and images were recorded after different incubation time. Control samples without H_2O_2 (*A–D*) and with 0.5 mM H_2O_2 (*E–H*) and 10 mM H_2O_2 (*I–L*) are shown. Markers for cell shape alterations were not observed. Scale bars = 20 μm.

visible shape alterations in intact RBCs, consistent with their unusually high antioxidant capacity (32). It is also possible that H_2O_2 is effectively neutralized by plasma proteins (e.g., albumin), although the antioxidant properties of turtle plasma have not been investigated. We also find that HbA polymers are able to bind O_2 cooperatively and with the same O_2 affinity and ATP sensitivity as the isolated HbA tetramer (Table 1). This finding indicates that, even in extreme cases of extensive HbA polymerization within turtle RBCs, blood O_2 transport would not be impaired under oxidative stress, namely under conditions where the turtle needs to resume normal respiration and metabolic activity after a period of O_2 deprivation.

The linear nature of the polymer itself may also explain the observed lack of RBC change in shape after H_2O_2 incubations (Fig. 9). Micrographs of purified HbA polymers (Fig. 6) show long and short chains of tetramers. These polymers are more flexible than the long and rigid helical structure of human mutant HbS (9) that causes the distinctive "sickle cell" distortion of RBCs. In contrast to turtle HbA, polymerization of human HbS is reversible and promoted by the protein conformational change following heme deoxygenation and does not involve disulfide bonds.

In contrast to HbA, the isoform HbD, coexpressed with HbA in turtle RBCs, is not able to form disulfide polymers (Fig. 2), consistent with the replacement of Cys with Asp at position 5 in the α^D-subunit, whereas all other Cys residues also present in HbA are conserved (8). Interestingly, in the chicken, also expressing HbA and HbD isoforms homologous to those of turtles, HbA is invariantly tetrameric while HbD may self-associate to large complexes upon deoxygenation (7, 27, 28). In this process, however, polymerization does not occur via disulfide bonds, despite the presence of external Cys residues (7, 14), indicating that Cys position and nearby residues at protein-protein contact interfaces are important for polymerization. Whether other bird and reptilian homologous HbD isoforms, including that of the freshwater turtle, may reversibly self-associate at high concentrations when deoxygenated remains to be investigated. Remarkably, in all cases where polymerization has been examined, disulfide-dependent Hb polymerization does not affect O_2 binding, as found here in the turtle and earlier in a teleost fish (11), mouse (34), and dwarf caiman (44). In contrast, reversible deoxygenation-dependent HbD polymerization as in the chicken may cause very high cooperativity of O_2 binding (7, 27, 28), reflecting functional interactions between Hb tetramers in addition to structural ones.

Perspectives and Significance

In conclusion, turtle HbA takes part to the RBC protein redox system involved in ROS detoxification via its redox

active Cys5α^A residue, together with the thioredoxin and glutaredoxin systems (16, 22). Because of the very high Hb concentration in RBCs, even the presence of a single additional reactive Cys in the Hb sequence may provide a convenient way of enhancing the cellular antioxidant capacity by millimolar levels. In the case of the freshwater turtle, this particular thiol reactivity of HbA is biologically highly relevant, as this species is among the very few vertebrates tolerant of severe hypoxia and anoxia and oxidative stress (2). Additionally, specific oxidation of Cys5α^A in turtle HbA by a major ROS, such as H_2O_2, appears to be strategically located in the molecule, as it generates fully functional Hb polymers with unaltered O_2 affinity, maintains RBC shape and thus does not interfere with blood O_2 transport. Other Cys residues highly conserved in vertebrate Hbs, such as Cys93β in reptile (including *T. scripta* HbA and HbD), bird, and mammal Hbs, may also potentially be involved in redox buffering and signaling (32), although their functional role cannot be inferred solely on the basis of amino acid sequence homology, as shown in this study.

ACKNOWLEDGMENTS

We thank Elin. E. Petersen and Catherine Williams (Department of Bioscience, Aarhus University) for assistance in the laboratory work and in blood sampling, respectively. We also thank three anonymous reviewers for useful comments on the manuscript.

GRANTS

The research was funded by grants from the Danish Council for Independent Research (4181–00094 to A. Fago). M. M. Golas acknowledges funding by the Lundbeck Foundation, and B. Sander acknowledges support by the Villum Foundation, Centre for Stochastic Geometry, and Advanced Bioimaging.

DISCLOSURES

No conflicts of interest, financial or otherwise, are declared by the authors.

AUTHOR CONTRIBUTIONS

A.G.P., S.V.P., and A.F. conceived and designed research; A.G.P., S.V.P., S.F., and SD performed experiments; A.G.P., S.V.P., S.F., and SD analyzed data; A.G.P., S.V.P., S.F., S.D., M.M.G., B.S., and A.F. interpreted results of experiments; A.G.P., S.V.P., and A.F. prepared figures; A.G.P. and A.F. drafted manuscript; A.G.P., S.V.P., S.F., S.D., M.M.G., B.S., and A.F. edited and revised manuscript; A.G.P., S.V.P., S.D., M.M.G., B.S., and A.F. approved final version of manuscript.

REFERENCES

1. **Bartlett GR.** Phosphate compounds in reptilian and avian red blood cells; developmental changes. *Comp Biochem Physiol* 61A: 191–202, 1978. doi:10.1016/0300-9629(78)90095-6.
2. **Bickler PE, Buck LT.** Hypoxia tolerance in reptiles, amphibians, and fishes: life with variable oxygen availability. *Annu Rev Physiol* 69: 145–170, 2007. doi:10.1146/annurev.physiol.69.031905.162529.
3. **Bury AF.** Analysis of protein and peptide mixtures. *J Chromatogr A* 213: 491–500, 1981. doi:10.1016/S0021-9673(00)80500-2.
5. **De Carlo S, Harris JR.** Negative staining and cryo-negative staining of macromolecules and viruses for TEM. *Micron* 42: 117–131, 2011. doi:10.1016/j.micron.2010.06.003.
6. **Chiancone E.** Dissociation of hemoglobin into subunits. II. Human oxyhemoglobin: gel filtration studies. *J Biol Chem* 243: 1212–1219, 1968.
7. **Cobb JA, Manning D, Kolatkar PR, Cox DJ, Riggs AF.** Deoxygenation-linked association of a tetrameric component of chicken hemoglobin. *J Biol Chem* 267: 1183–1189, 1992.
8. **Damsgaard C, Storz JF, Hoffmann FG, Fago A.** Hemoglobin isoform differentiation and allosteric regulation of oxygen binding in the turtle, *Trachemys scripta*. *Am J Physiol Regul Integr Comp Physiol* 305: R961–R967, 2013. doi:10.1152/ajpregu.00284.2013.
9. **Dykes G, Crepeau RH, Edelstein SJ.** Three-dimensional reconstruction of the fibres of sickle cell haemoglobin. *Nature* 272: 506–510, 1978. doi:10.1038/272506a0.
10. **Erickson HP.** Size and shape of protein molecules at the nanometer level determined by sedimentation, gel filtration, and electron microscopy. *Biol Proced Online* 11: 32–51, 2009. doi:10.1007/s12575-009-9008-x.
11. **Fago A, Romano M, Tamburrini M, Coletta M, D'Avinno R, Di Prisco G.** A polymerising Root-effect fish hemoglobin with high subunit heterogeneity. Correlation with primary structure. *Eur J Biochem* 218: 829–835, 1993. doi:10.1111/j.1432-1033.1993.tb18438.x.
12. **Bunn HF.** Pathogenesis and treatment of sickle cell disease. *N Engl J Med* 337: 762–769, 1997. doi:10.1056/NEJM199709113371107.
13. **Frische S, Bruno S, Fago A, Weber RE, Mozzarelli A.** Oxygen binding by single red blood cells from the red-eared turtle *Trachemys scripta*. *J Appl Physiol (1985)* 90: 1679–1684, 2001.
14. **Hermes-Lima M, Zenteno-Savín T.** Animal response to drastic changes in oxygen availability and physiological oxidative stress. *Comp Biochem Physiol C Toxicol Pharmacol* 133: 537–556, 2002. doi:10.1016/S1532-0456(02)00080-7.
15. **Herold S, Rehmann FJK.** Kinetic and mechanistic studies of the reactions of nitrogen monoxide and nitrite with ferryl myoglobin. *J Biol Inorg Chem* 6: 543–555, 2001. doi:10.1007/s007750100231.
16. **Holmgren A.** Thioredoxin and glutaredoxin systems. *J Biol Chem* 264: 13963–13966, 1989.
17. **Jackson DC.** Living without oxygen: lessons from the freshwater turtle. *Comp Biochem Physiol A Mol Integr Physiol* 125: 299–315, 2000. doi:10.1016/S1095-6433(00)00160-4.
18. **Jacobsen SB, Hansen MN, Jensen FB, Skovgaard N, Wang T, Fago A.** Circulating nitric oxide metabolites and cardiovascular changes in the turtle Trachemys scripta during normoxia, anoxia and reoxygenation. *J Exp Biol* 215: 2560–2566, 2012. doi:10.1242/jeb.070367.
19. **Janecka JE, Nielsen SSE, Andersen SD, Hoffmann FG, Weber RE, Anderson T, Storz JF, Fago A.** Genetically based low oxygen affinities of felid hemoglobins: lack of biochemical adaptation to high-altitude hypoxia in the snow leopard. *J Exp Biol* 218: 2402–2409, 2015. doi:10.1242/jeb.125369.
20. **Jensen B, Storz JF, Fago A.** Bohr effect and temperature sensitivity of hemoglobins from highland and lowland deer mice. *Comp Biochem Physiol A Mol Integr Physiol* 195: 10–14, 2016. doi:10.1016/j.cbpa.2016.01.018.
21. **Koldkjaer P, McDonald MD, Prior I, Berenbrink M.** Pronounced in vivo hemoglobin polymerization in red blood cells of Gulf toadfish: a general role for hemoglobin aggregation in vertebrate hemoparasite defense? *Am J Physiol Regul Integr Comp Physiol* 305: R1190–R1199, 2013. doi:10.1152/ajpregu.00246.2013.
22. **Kowaltowski AJ, de Souza-Pinto NC, Castilho RF, Vercesi AE.** Mitochondria and reactive oxygen species. *Free Radic Biol Med* 47: 333–343, 2009. doi:10.1016/j.freeradbiomed.2009.05.004.
23. **Moncada S, Erusalimsky JD.** Does nitric oxide modulate mitochondrial energy generation and apoptosis? *Nat Rev Mol Cell Biol* 3: 214–220, 2002. doi:10.1038/nrm762.
24. **Nikinmaa M.** *Vertebrate Red Blood Cells*. Berlin, Germany: Springer-Verlag, 1990. doi:10.1007/978-3-642-83909-2.
25. **Patterson SD, Katta V.** Prompt fragmentation of disulfide-linked peptides during matrix-assisted laser desorption ionization mass spectrometry. *Anal Chem* 66: 3727–3732, 1994. doi:10.1021/ac00093a030.
26. **Poole LB.** The basics of thiols and cysteines in redox biology and chemistry. *Free Radic Biol Med* 80: 148–157, 2015. doi:10.1016/j.freeradbiomed.2014.11.013.
27. **Rana MS, Knapp JE. Holland RA, Riggs AF.** Component D of chicken hemoglobin and the hemoglobin of the embryonic tammar wallaby (*Macropus eugenii*) self-associate upon deoxygenation: effect on oxygen binding. *Proteins* 70: 553–5619, 2008. doi:10.1002/prot.21793.
28. **Rana MS, Riggs AF.** Indefinite noncooperative self-association of chicken deoxy hemoglobin D. *Proteins* 79: 1499–1512, 2011. doi:10.1002/prot.22978.
29. **Reczek CR, Chandel NS.** ROS-dependent signal transduction. *Curr Opin Cell Biol* 33: 8–13, 2015. doi:10.1016/j.ceb.2014.09.010.
30. **Reischl E.** High sulfhydryl content in turtle erythrocytes: is there a relation with resistance to hypoxia? *Comp Biochem Physiol B* 85: 723–726, 1986. doi:10.1016/0305-0491(86)90167-7.
31. **Reischl E.** Sulfhydryl-rich hemoglobins in reptiles: a defense against reactive oxygen species? In: *Nonmammalian Animal Models for Biochemical Research*. Boca Raton, FL: CRC, 1989, p. 309–318.

32. **Reischl E, Dafre AL, Franco JL, Wilhelm Filho D.** Distribution, adaptation and physiological meaning of thiols from vertebrate hemoglobins. *Comp Biochem Physiol C Toxicol Pharmacol* 146: 22–53, 2007. doi:10.1016/j.cbpc.2006.07.015.
33. **Reischl E, Höhn M, Jaenicke R, Bauer C.** Bohr effect, electron spin resonance spectroscopy and subunit dissociation of the hemoglobin components from the turtle *Phrynops hilarii*. *Comp Biochem Physiol B* 78: 251–257, 1984. doi:10.1016/0305-0491(84)90179-2.
34. **Riggs A, Rona M.** The oxygen equilibria and aggregation behavior of polymerizing mouse hemoglobins. *Biochim Biophys Acta* 175: 248–259, 1969. doi:10.1016/0005-2795(69)90003-8.
35. **Shevchenko A, Tomas H, Havlis J, Olsen JV, Mann M.** In-gel digestion for mass spectrometric characterization of proteins and proteomes. *Nat Protoc* 1: 2856–2860, 2007. doi:10.1038/nprot.2006.468.
36. **Sies H.** Role of metabolic H_2O_2 generation: redox signaling and oxidative stress. *J Biol Chem* 289: 8735–8741, 2014. doi:10.1074/jbc.R113.544635.
37. **Sullivan B, Riggs A.** Structure, function and evolution of turtle hemoglobins. II. Electrophoretic studies. *Comp Biochem Physiol* 23: 449–458, 1967. doi:10.1016/0010-406X(67)90398-2.
38. **Sullivan B, Riggs A.** The subunit dissociation properties of turtle hemoglobins. *Biochim Biophys Acta* 140: 274–283, 1967. doi:10.1016/0005-2795(67)90468-0.
39. **Tondo C, Bonaventura J, Bonaventura C, Brunori M, Amiconi G, Antonini E.** Functional properties of hemoglobin Pôrto Alegre ($\alpha_2{}^{A}\beta_2{}^{9Ser\rightarrow Cys}$) and the reactivity of its extra cysteinyl residue. *Biochim Biophys Acta* 342: 15–20, 1974. doi:10.1016/0005-2795(74)90101-9.
40. **Tufts DM, Natarajan C, Revsbech IG, Projecto-Garcia J, Hoffmann FG, Weber RE, Fago A, Moriyama H, Storz JF.** Epistasis constrains mutational pathways of hemoglobin adaptation in high-altitude pikas. *Mol Biol Evol* 32: 287–298, 2015. doi:10.1093/molbev/msu311.
41. **Ultsch GR.** Ecology and physiology of hibernation and overwintering among freshwater fishes, turtles, and snakes. *Biol Rev Camb Philos Soc* 64: 435–515, 1989. doi:10.1111/j.1469-185X.1989.tb00683.x.
42. **Van Assendelft OW.** *Spectrophotometry of Haemoglobin Derivatives*. Assen, The Netherlands: Royal VanGorcum, 1970.
43. **Weber RE.** Use of ionic and zwitterionic (Tris/BisTris and HEPES) buffers in studies on hemoglobin function. *J Appl Physiol (1985)* 72: 1611–1615, 1992.
44. **Weber RE, Fago A, Malte H, Storz JF, Gorr TA.** Lack of conventional oxygen-linked proton and anion binding sites does not impair allosteric regulation of oxygen binding in dwarf caiman hemoglobin. *Am J Physiol Regul Integr Comp Physiol* 305: R300–R312, 2013. doi:10.1152/ajpregu.00014.2013.